



# Distributed host-based collaborative detection for false data injection attacks in smart grid cyber-physical system



Beibei Li<sup>a</sup>, Rongxing Lu<sup>b,\*</sup>, Wei Wang<sup>a</sup>, Kim-Kwang Raymond Choo<sup>c,d</sup>

<sup>a</sup> School of Electrical and Electronic Engineering, Nanyang Technological University, 50 Nanyang Avenue, Singapore 639798, Singapore

<sup>b</sup> Faculty of Computer Science, University of New Brunswick, Fredericton, Canada E3B 5A3

<sup>c</sup> Department of Information Systems and Cyber Security, University of Texas at San Antonio, San Antonio, TX 78249, USA

<sup>d</sup> School of Information Technology & Mathematical Sciences, University of South Australia, Adelaide, SA 5001, Australia

## HIGHLIGHTS

- A rule specification-based collaborative false data detection method is proposed.
- A reputation system with an adaptive reputation updating algorithm is devised.
- Distributed detection significantly mitigates control center's computation burden.
- The effectiveness of the proposal is demonstrated by real-time measurement data.

## ARTICLE INFO

### Article history:

Received 2 September 2016

Received in revised form

10 November 2016

Accepted 4 December 2016

Available online 23 December 2016

### Keywords:

Smart grid cyber-physical system (CPS)

False data injection attack

Distributed host-based collaborative detection

Adaptive reputation system

## ABSTRACT

False data injection (FDI) attacks are crucial security threats to smart grid cyber-physical system (CPS), and could result in cataclysmic consequences to the entire power system. However, due to the high dependence on open information networking, countering FDI attacks is challenging in smart grid CPS. Most existing solutions are based on state estimation (SE) at the highly centralized control center; thus, computationally expensive. In addition, these solutions generally do not provide a high level of security assurance, as evidenced by recent work that smart FDI attackers with knowledge of system configurations can easily circumvent conventional SE-based false data detection mechanisms. In this paper, in order to address these challenges, a novel distributed host-based collaborative detection method is proposed. Specifically, in our approach, we use a conjunctive rule based majority voting algorithm to collaboratively detect false measurement data inserted by compromised phasor measurement units (PMUs). In addition, an innovative reputation system with an adaptive reputation updating algorithm is also designed to evaluate the overall running status of PMUs, by which FDI attacks can be distinctly observed. Extensive simulation experiments are conducted with real-time measurement data obtained from the PowerWorld simulator, and the numerical results fully demonstrate the effectiveness of our proposal.

© 2016 Elsevier Inc. All rights reserved.

## 1. Introduction

Smart grid cyber-physical system (CPS) is designed to facilitate highly efficient, accurate, and reliable power delivery as well as sustainable energy integration and utilization [22,40]. Despite the potential benefits of a smart grid CPS, there are underlying threats that could jeopardize the security of the system and consequently,

have a cascading effect on the stability of the society [22,9,17,21] (see Fig. 1 the system view of a smart grid CPS).

In recent times, a number of high profile incidents targeting smart grid as well as other CPSs have been reported, e.g., Stuxnet [12], Conficker [36], and US drones hack [14]. Malicious attackers may attempt to falsify sensor measurements, embed fake control commands, delay or drop sensor readings or control commands [22,1,13,8]. False data injection (FDI) attacks are increasingly recognized as a serious threat to smart grid CPS, and unsurprisingly, have been the focus of computer security researchers and industry practitioners. FDI attacks and mitigation strategies on smart grid CPS have been also evolved over the years. Conventional false data detection (FDD) approaches are generally based on

\* Corresponding author.

E-mail addresses: [blili012@e.ntu.edu.sg](mailto:blili012@e.ntu.edu.sg) (B. Li), [rlu1@unb.ca](mailto:rlu1@unb.ca) (R. Lu), [wei001@e.ntu.edu.sg](mailto:wei001@e.ntu.edu.sg) (W. Wang), [raymond.choo@fulbrightmail.org](mailto:raymond.choo@fulbrightmail.org) (K.-K.R. Choo).

<http://dx.doi.org/10.1016/j.jpdc.2016.12.012>

0743-7315/© 2016 Elsevier Inc. All rights reserved.

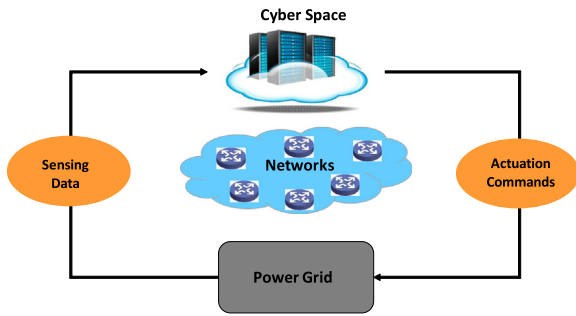


Fig. 1. The system view of a smart grid CPS.

system state estimation (SE) [24,7,18]. However, Liu et al. in [23] showed that smart FDI attackers armed with the knowledge of system configurations could easily bypass the traditional SE-based FDD schemes without detection. Consequently, existing FDD approaches may be ineffective against newer or emerging FDI attacks. The major limitation of legacy FDD schemes is that they mainly focus on the inter-correlations among the measurement data (e.g., residuals and errors), rather than the malicious behaviors of meter devices, such as phasor measurement units (PMUs) and smart meters. Furthermore, in existing literature FDD is generally performed by the power system's centralized control center (CC), due to the demanding computational requirements [7,18]. Although a small number of hierarchical or distributed FDD schemes are designed to reduce the computation requirements at the CC [2,26], most of them are still based on SE; thus, vulnerable to smart attackers. Another limitation of legacy FDD methods is that some prevailing countermeasures against cyber intrusion only aim to detect the “bad” data without further evaluating the true running status of the meter devices that might already be compromised by malicious attackers [24,2,15]. These undetected hidden attackers can continue to launch or improve their attacks subsequently. Therefore, countering against FDI attacks in smart grid CPS remains a research challenge, and one that we seek to address in this paper.

Thus, we propose a distributed host-based collaborative detection (DHCD) method based on rule specifications, rather than SE. DHCD can not only reduce the computational burden of the CC, but also achieve fast FDD and the capability to evaluate the running status of meter devices. Specifically, in our method, each PMU is assigned a host monitor (HM) serving as the distributed local false data detector. Based on a set of pre-defined rule specifications, the monitors determine the anomalous levels of measurement data collected by their supervised PMUs. Then, by sharing and comparing the anomalous levels of the measurement data collected by the neighboring interconnected PMUs, these interconnected monitors collaboratively make a decision based on the majority voting algorithm to determine whether their own measurement data is falsified. To evaluate the overall running status of the PMUs, a reputation system with an adaptive reputation updating (ARU) algorithm is designed, where a malfunction of PMU can be easily identified. The contributions of our work are summarized as follows:

1. We develop a DHCD method to detect FDI attacks in smart grid CPS based on rule specifications, which can be used to effectively mitigate smart FDI attacks.
2. Our method can not only achieve fast and high accuracy of FDD, but also allow the identification of compromised PMUs using our designed reputation system.
3. Our distributed detection method will “displace” the computational burden of the CC by delegating FDD tasks to the local monitors.

The remainder of this paper is organized as follows. Section 2 reviews the related literature. Section 3 presents the system model, the threat model, and our design goals. The DHCD method is detailed in Section 4, followed by the performance evaluation in Section 5. Section 6 concludes the paper with future research directions.

## 2. Related work

Intrusion detection has been extensively studied in the literature [30,16], including for smart grids [22,1,8], wireless sensor networks [19,34,39], mobile ad hoc networks [27], etc.

Since the seminal work of Schweppe et al. who proposed a static SE-based approach to detect bad data in electric power systems [35], FDD has been the focus of research in the power system industry. Over the years, a number of FDD approaches based on SE designed to mitigate FDI attacks in smart grid CPS have been proposed [24,7,15]. For example, Merrill and Schweppe presented a bad data suppression estimator based on a non-quadratic cost function to improve the performance of static SE [24]. Handschin et al. presented a method to detect and identify the bad data and structural error problems, and improved bad data analysis (detection probability, and effects of bad data) [15]. Cutsem et al. also proposed an identification method attempting to alleviate some existing difficulties, such as multiple and interacting bad data [10].

However, Liu et al. demonstrated that a new class of smart attackers armed with the knowledge of system configurations were capable of constructing a set of falsified data to circumvent the legacy SE-based FDD mechanisms [23]. Xie et al. also explained that some potential attackers were able to launch FDIs in deregulated electricity markets [40]. Thus, a small number of detection methods have been proposed to identify such “undetectable” attackers. Pasqualetti proposed a unified framework and advanced monitoring procedure to detect malfunctions or measurement corruptions of network components caused by an omniscient adversary [28]. Bobba et al. attempted to detect smart FDI attacks by protecting a strategically selected set of sensor measurements and finding a way to independently verify or measure these measurements [3].

Rather than using the static SE and to fully leverage the features of meter devices' anomalous behaviors, our proposed DHCD method mitigates FDIs by establishing a rule specification based behavior model and collaboratively verifying the measurement data. In addition, we design a novel reputation system with an ARU algorithm to evaluate the running status of PMUs, by which FDI attacks can be easily observed. Furthermore, our distributed detection system can significantly enhance the efficiency of FDD tasks.

## 3. Models and design goals

In this section, we introduce the system model, the threat model, and our design goals.

### 3.1. System model

A smart grid CPS is a fully automated system capable of achieving self-healing, cost reduction, improved reliability and efficiency. These promising benefits are intensively grounded on the wide area measurement and control system (WAMCS), as it can provide high-level observability and controllability in power system operations [20,32,33]. Thus, in this paper, we consider the WAMCS as our system model.

As shown in Fig. 2, WAMCS is an integrated system consisting of PMUs, phasor data concentrators (PDCs), heterogeneous communication networks, and a CC. Specifically, PMUs, located at the substations of the power generation and transmission system, are

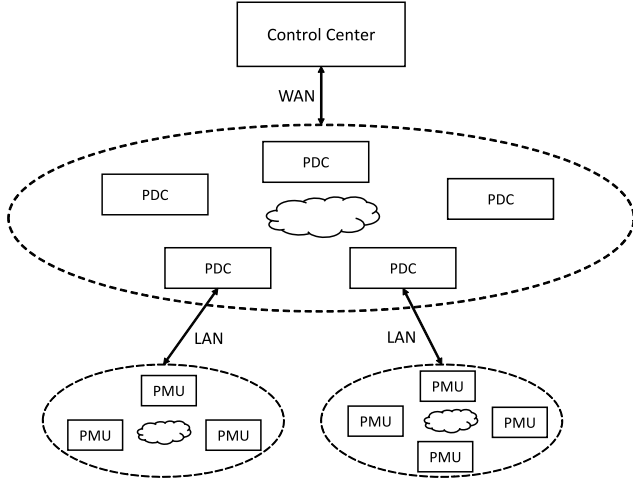


Fig. 2. The architecture of wide area measurement and control system.

capable of measuring the real-time status of the power system. For example, the real-time amplitude and phase angle of voltage at the bus, of current on the transmission line, and of the power at each branch, can be measured by the PMUs. These measurement data are then periodically transmitted to the PDCs, usually in 50 Hz, through the local area network (LAN). Then, the aggregated data at the PDCs are delivered to the CC via the wide area network (WAN) for further data analysis, such as state estimation, event diagnostics, and contingency analysis.

### 3.2. Threat model

The real-time data provided by PMUs serve as the basis for automated, efficient, and reliable system control. However, adversaries seeking to intervene or manipulate system operations can attempt to inject false measurement data through compromised PMUs. Successful FDI attack may compromise the above-mentioned promising functionalities or even jeopardize the system operations.

In our threat model, we consider that PMUs in the WAMCS can be compromised by FDI attackers (e.g., rewriting the program settings, or stealing the secret information for data communication). Note that, in smart grid CPS, a single piece of false measurement data may not have significant impact on system operations, because the system is capable of correcting trivial faults or mistakes. However, the system may not be able to auto-correct in the event that consecutive false measurement data are received; consequently, resulting in system failures. As such, to successfully launch an FDI attack in practice, attackers usually recklessly and persistently inject false measurement data once they have an opportunity. This is the behavior pattern of FDI attackers we consider in the threat model.

### 3.3. Design goals

Based on the aforementioned system model and threat model, our design goals are to develop an accurate, efficient, and scalable FDD method in smart grid CPS. Specifically, the following specific objectives should be achieved.

**Accuracy:** The devised method is able to effectively detect smart FDI attacks, achieving both high detection rate and low false alarm rate.

**Efficiency:** The detection method should not introduce additional computational burden to the system, particularly to the CC inherent in traditional FDD schemes.

**Scalability:** The smart grid CPS needs to be scalable (similar to a cloud system) by allowing new devices to be added, etc., without incurring expensive (financial) costs.

## 4. Proposed DHCD method

In this section, we present the proposed DHCD method, which is composed of two steps (subsections): collaborative FDD and determination of compromised PMU. In the first step, we employ a set of rule specifications to identify anomalous measurement data reported by the PMU. Then, in the second step, we devise a reputation system with an ARU algorithm to monitor and assess PMUs' overall behaviors in order to further detect compromised PMU.

### 4.1. Collaborative FDD

In normal operational circumstances, the power grid operates in a stable status. In other words, all state variables vary in a mutual balanced manner according to Kirchhoff's law, demand-response constraints, etc. As such, any change of a variable state on one bus or transmission line, resulting from either the normal demand variation or system faults, would lead to corresponding state changes of the same and/or other variables on interconnected buses or transmission lines. For example, as shown in Fig. 3, the contouring maps with comparison are plotted, which describe the distribution of the current amplitude on each transmission line (a) before and (b) after an open circuit event on transmission line from Bus 16 to Bus 17. As shown in Fig. 3(b), after the occurrence of this open circuit event, the current amplitude values near Line 16 to 17 shift. The closer to this line, the more the value changes.

In contrast, if only some changes of variable states occur on one bus, without a corresponding shift in the parallel variables of interconnected buses, such changes can be regarded as anomalous. These anomalies may originate from either malfunction of PMU devices or malicious activities due to compromised PMUs. In this paper, we only consider possible malicious activities rather than device malfunction, as there are many existing approaches to address issues relating to device malfunction. Based on the inter-correlations of power systems, we design a collaborative detection method to detect anomalous measurement data reported by PMUs [6,29].

#### 4.1.1. Normal rule specifications

When power system is under normal operation, all state variables must naturally follow some constraints and hold some properties. Let us take active power  $P$  as an example, which should obey the following rules:

- $P_{\min} < P^t < P_{\max}$ :  $P$  at any time under stable status must vary within an experienced range  $[P_{\min}, P_{\max}]$ .
- $|P^t - P^{t-1}| < P_{\Delta}$ : The variation of  $P$  within one time interval should be less than an experienced threshold  $P_{\Delta}$ .
- $|P_{in}^t - P_{out}^t| < P_{loss}$ : The difference of  $P$  flowing into a bus and flowing out the bus ought to be less than an experienced power loss threshold  $P_{loss}$ .
- Other more complicated rules.

As such, we pre-define some rule specifications as listed in Table 1 that PMUs have to coincide with in the stable status. These rule specifications serve as the basis of our method to identify the anomalous measurement data (for convenience, the superscript  $t$  is omitted).

To represent the results of whether the rule specifications have been violated, we employ a binary system, where "0" denotes that the measurement data of one variable follows the relevant rule specification and "1" indicates a violation. A binary sequence with length  $E$  ( $E$  is the number of rule specifications, and here  $E$  is 4) is utilized to represent the conjunctive results pertaining to the entire measurement data. For instance, "1001" denotes that both rules 1 and 4 are violated. A non violation of the conjunctive four

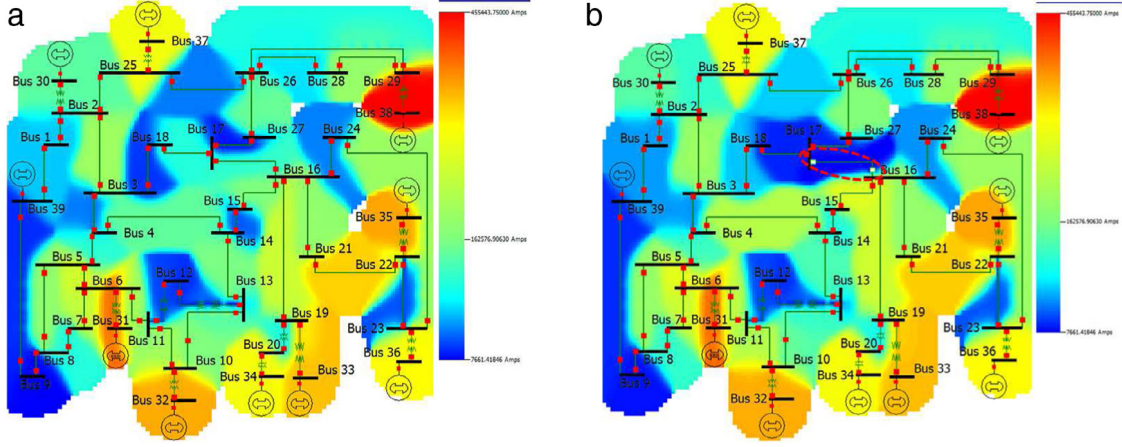


**Fig. 3.** Comparison of contouring maps describing the distribution of current amplitude on transmission lines: (a) before open circuit and (b) after open circuit on line from Bus 16 to 17 (marked by a red circle) in IEEE-39 bus system. As the bar shows, red area denotes high current amplitude while blue area denotes low current amplitude. (For interpretation of the references to color in this figure legend, the reader is referred to the web version of this article.)

**Table 1**  
Rules specifications for PMUs in stable status.

Index	Variable	Rule description
1	Active power angle	$\Delta\delta < \delta_\Delta$
2	(Phase A) voltage amplitude	$\Delta V < V_\Delta$
3	Load Mvar	$\Delta L_{Mvar} < L_{Mvar\Delta}$
4	Load MW	$\Delta L_{MW} < L_{MW\Delta}$

rule specifications is represented by “0000”, which is our *baseline* of PMUs’ behaviors.

In order to assess to what extent each piece of measurement data is anomalous, we introduce a normalized Euclidean distance strategy to determine the *anomalous level*  $l^t$ , which is shown as follows:

$$l^t = D_0(seq^t, seq_0), \quad (1)$$

where  $seq^t$  is the binary sequence representing the conjunctive results of measurement data at time  $t$ , while  $seq_0 = “0000”$  is the baseline.  $D_0$  is the normalized Euclidean distance of the two sequences  $seq^t$  and  $seq_0$ . Euclidean distance is the square root of the sum of results that are different between two sequences. For example, the Euclidean distance between sequence “1001” and the baseline “0000” is  $\sqrt{1^2 + 0 + 0 + 1^2} \approx 1.414$ . Then, the *anomalous level*  $l$  is computed by the normalized distance, i.e.,  $1.414/\sqrt{1^2 + 1^2 + 1^2 + 1^2} \approx 0.707$ .

#### 4.1.2. FDD algorithm with iterative majority voting

Fig. 4 shows the distributed host-based collaborative FDD system, where each host monitor (HM) is responsible for monitoring and assessing the behaviors of its administrated PMU. Let  $\mathcal{M} = \{M_1, M_2, \dots, M_N\}$  denote the set of monitors and  $\mathcal{U} = \{U_1, U_2, \dots, U_N\}$  the set of PMUs, where  $N$  is the total number of HMs or PMUs. HMs communicate among each other following the connection pattern of the PMUs, which means each HM only communicates with HMs that their monitored PMUs have interconnection relations.

As stated above, we utilize the inter-correlations between the state variables to build our detection method. Algorithm 1 outlines the FDD algorithm with iterative majority voting process. Concretely, set  $\mathcal{M}$  is initialized as  $\mathcal{M} = \{M_1, M_2, \dots, M_N\}$ , and a flag variable *repeat\_flag* as “0”. Note that *repeat\_flag* = “0” indicates that the procedure does not need to be repeated, while *repeat\_flag* = “1” indicates the need to repeat the procedure. Next, each monitor  $M_i \in \mathcal{M}$  determines the conjunctive result  $R_i^t$  of current piece of measurement data, and broadcasts the result to

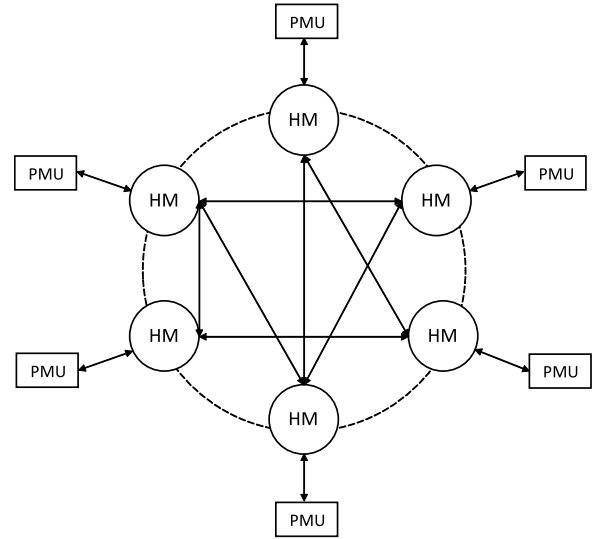


**Fig. 4.** The distributed host-based collaborative FDD system.

$M_1 :$	Rule_Index	R1	R2	R3	R4
	Rule_Result	0	0	0	0
$M_2 :$	Rule_Index	R1	R2	R3	R4
	Rule_Result	0	0	0	1
$\vdots$					
$M_N :$	Rule_Index	R1	R2	R3	R4
	Rule_Result	0	1	0	0

**Fig. 5.** An example of the conjunctive results transmitted between HMs.

neighboring connected monitors  $\mathcal{M}_i = \{M_j | M_j \sim M_i\}$ . An example is shown in Fig. 5.



Then,  $M_i$  launches the false data identification process. If there is no bit “1” in the result  $R_i^f$ , then no false data is detected. Otherwise,  $M_i$  needs to determine how many of its connected monitors have a bit “1” in their conjunctive results  $R_j^f$ . If more than or equal to half of the connected monitors have a bit “1” at the same position in  $R_i^f$ ,  $M_i$  concludes that  $U_i$  has reported a piece of false measurement data; otherwise,  $R_i^f$  is tentatively considered suspicious. After all  $M_i \in \mathcal{M}$  have concluded the first procedure, the termination criterion is determined. If  $\text{repeat\_flag} == “1”$ , this procedure is repeated to further identify the false data; otherwise, the procedure goes to the end.

---

**Algorithm 1** FDD Algorithm

---

```

1: initialization:  $\mathcal{M} = \{M_1, M_2, \dots, M_N\}$ ,  $\text{Upperbound} = 5$ ,  $\text{Iteration} = 0$ ,  $\text{repeat\_flag} = “0”$ 
2: procedure
3:   for each monitor  $M_i \in \mathcal{M}$  do
4:     (1). determines the conjunctive result  $R_i^f$  of current piece of measurement data.
5:     (2). broadcasts the result  $R_i^f$  to the neighboring connected monitors  $\mathcal{M}_i = \{M_j | M_j \sim M_i\}$ .
6:     (3). identifies false data:
7:       if there is no bit “1” in the result  $R_i^f$  then
8:         output: no false data detected.
9:       else if more than or equal to half of the monitors in  $\mathcal{M}_i$  hold bit “0” at the same position in the result  $R_i^f$  then
10:        (a). output: false data detected.
11:        (b). removes  $M_i$  from  $\mathcal{M}$  and its connections with other monitors.
12:       else
13:        (a). keeps  $R_i^f$  as suspicious result.
14:        (b).  $\text{repeat\_flag} = “1”$ .
15:       end if
16:   end for
17:   (4). judgets the termination criteria:
18:   if  $\text{repeat\_flag} == “1”$  and  $\text{Iteration} < \text{Upperbound}$  then
19:     (a). repeats procedure.
20:     (b).  $\text{Iteration} = \text{Iteration} + 1$ .
21:   else
22:     ends the procedure.
23:   end if
24: end procedure

```

---

#### 4.2. Determination of compromised PMU

FDD step is a critical process to detect false data, but it is not sufficient to identify compromised PMUs. Therefore, in the second step, we employ a reputation-based algorithm to monitor and assess the PMUs’ overall behaviors over a period of time, which allows us to identify compromised PMUs if their reputation level drops below an acceptable threshold [11,31].

Specifically, in this subsection, we first model the probability distribution of the anomalous level of measurement data with a Beta distribution. Then, we estimate its two shape parameters  $\alpha$  and  $\beta$  using maximum likelihood estimation (MLE) and Newton–Raphson method. Then, a detailed description of an adaptive reputation updating (ARU) algorithm is presented.

##### 4.2.1. Probability distribution of anomalous level

Let random variable  $X$  be the anomalous level of a piece of measurement data, where  $X$  can either be 0 or 1 and it is determined by the normalized Euclidean distance (see Section 4.1.1). Particularly,  $X = 0$  represents compliance of the rule specifications, while  $X = 1$  represents a violation. Here, to determine the exact distribution of the probabilities of different anomalous level and its future

values, we model the random variable  $X$  using a  $Beta(\alpha, \beta)$  distribution. Beta distribution family can represent a collection of probability distributions, and can be used to depict a prior distribution of an unknown distribution with only a series of collected observations.

The probability density function (pdf) of a Beta distribution is

$$f(x; \alpha, \beta) = \frac{\Gamma(\alpha + \beta)}{\Gamma(\alpha)\Gamma(\beta)} x^{\alpha-1}(1-x)^{\beta-1}, \quad (2)$$

where  $\alpha$  and  $\beta$  are the two shape parameters. The mean value of a Beta distribution is

$$\mu = E[X] = \int_0^1 x \frac{\Gamma(\alpha + \beta)}{\Gamma(\alpha)\Gamma(\beta)} x^{\alpha-1}(1-x)^{\beta-1} dx = \frac{\alpha}{\alpha + \beta}. \quad (3)$$

To obtain the exact distribution of  $X$ , we estimate the parameters  $\alpha$  and  $\beta$  using a well-known method MLE. We suppose that the  $n$  independent and identically distributed observations  $\{x_1, x_2, \dots, x_n\}$  are from an unknown distribution with pdf  $f_0(\cdot|\theta)$ ,  $\theta$  is a vector of parameters. As for our model, the Beta distribution,  $\theta = [\alpha \ \beta]$ . By using MLE, we formulate the joint density probability function of these  $n$  independent and identically distributed observations  $\{x_1, x_2, \dots, x_n\}$  as

$$f(x_1, x_2, \dots, x_n | \alpha, \beta) = \prod_{i=1}^n f(x_i | \alpha, \beta). \quad (4)$$

Now we look at this equation from a different perspective by fixing the observed samples  $\{x_1, x_2, \dots, x_n\}$  of this function, then  $\alpha, \beta$  are the variables of the function that we call the likelihood:

$$\mathcal{L}(\alpha, \beta | x_1, x_2, \dots, x_n) = \prod_{i=1}^n f(x_i | \alpha, \beta). \quad (5)$$

In most cases, it is easier to work with the natural logarithm of the likelihood function. We rewrite it as

$$\begin{aligned}
\ln \mathcal{L}(\alpha, \beta | x_1, x_2, \dots, x_n) &= \ln \prod_{i=1}^n f(x_i | \alpha, \beta) \\
&= \sum_{i=1}^n \ln \left\{ \frac{\Gamma(\alpha + \beta)}{\Gamma(\alpha)\Gamma(\beta)} x_i^{\alpha-1}(1-x_i)^{\beta-1} \right\} \\
&= n \ln \Gamma(\alpha + \beta) - n[\ln \Gamma(\alpha) + \ln \Gamma(\beta)] \\
&\quad + (\alpha - 1) \sum_{i=1}^n \ln x_i + (\beta - 1) \sum_{i=1}^n \ln(1 - x_i).
\end{aligned} \quad (6)$$

Then, we have to find the optimal values of  $\alpha$  and  $\beta$  that maximize  $\ln \mathcal{L}(\alpha, \beta | x_1, \dots, x_n)$ . Since logarithm is a strictly monotonically increasing function, the maximum value, if it exists, could be calculated by

$$\begin{cases} \frac{\partial \ln \mathcal{L}}{\partial \alpha} = 0 \\ \frac{\partial \ln \mathcal{L}}{\partial \beta} = 0. \end{cases} \quad (7)$$

That is

$$g_1(\alpha, \beta) = \psi(\alpha) - \psi(\alpha + \beta) - \frac{1}{n} \sum_{i=1}^n \ln x_i = 0 \quad (8)$$

$$g_2(\alpha, \beta) = \psi(\beta) - \psi(\alpha + \beta) - \frac{1}{n} \sum_{i=1}^n \ln(1 - x_i) = 0 \quad (9)$$

where  $\psi(x)$  is the digamma function defined as

$$\psi(x) = \frac{d}{dx} \ln \Gamma(x) = \frac{\Gamma'(x)}{\Gamma(x)}. \quad (10)$$

There is no closed-form solution to Eqs. (8) and (9), so we use the Newton–Raphson method to find the approximate roots. The parameters  $\hat{\theta} = [\hat{\alpha} \ \hat{\beta}]$  can be iteratively estimated by [4]

$$\hat{\theta}_{i+1} = \hat{\theta}_i - \frac{\mathbf{g}(\hat{\theta}_i)}{\mathbf{J}_{\mathbf{g}}(\hat{\theta}_i)}, \quad (11)$$

where  $\mathbf{g} = [g_1 \ g_2]$ , and  $\mathbf{J}_{\mathbf{g}}(\hat{\theta}_i)$  is an  $2 \times 2$  Jacobian matrix defined over the function vector  $\mathbf{g}(\hat{\theta}_i)$  defined as

$$\begin{bmatrix} \frac{dg_1}{d\alpha} & \frac{dg_1}{d\beta} \\ \frac{dg_2}{d\alpha} & \frac{dg_2}{d\beta} \end{bmatrix} \quad (12)$$

with

$$\frac{dg_1}{d\alpha} = \psi'(\alpha) - \psi'(\alpha + \beta) \quad (13)$$

$$\frac{dg_1}{d\beta} = \frac{dg_2}{d\alpha} = -\psi'(\alpha + \beta) \quad (14)$$

$$\frac{dg_2}{d\beta} = \psi'(\beta) - \psi'(\alpha + \beta). \quad (15)$$

This Newton–Raphson method converges when the estimates of  $\hat{\alpha}$  and  $\hat{\beta}$  change by less than an acceptable threshold with each successive iteration.

#### 4.2.2. ARU algorithm

With the exact probability distribution of the anomalous level, we can obtain its expectation value  $\mu$ , which is the best indicator of the overall performance of the PMUs over the observation period. Here, we define the history reputation level of a PMU as

$$T = 1 - \mu = \frac{\beta}{\alpha + \beta}. \quad (16)$$

While, a dependable reputation system should be able to adaptively adjust the reputation values according to dynamic behavioral changes [37]. Thus, in this paper, we incorporate the history reputation level and the subsequent behavior fluctuations of PMUs to assess their real-time reputation levels. In addition, adaptive parameters are used to allow different impacts due to the reputation levels with different behavior observations. The real-time reputation level of a PMU is then defined as

$$\begin{aligned} T^t &= \omega \cdot T_h + (1 - \omega) \cdot T_u^t \\ &= \omega \cdot \frac{\beta}{\alpha + \beta} + (1 - \omega) \cdot \frac{\lambda_g \cdot N_g^t + 1}{\lambda_g \cdot N_g^t + \lambda_b^t \cdot N_b^t + 1}, \end{aligned} \quad (17)$$

where  $T_h$  is the history reputation level of a PMU, and  $T_u^t$  is the updating reputation level at time instant  $t$ .  $\omega$  is the weight assigned for the history reputation level to evaluate the importance of history experience to the real-time reputation level, while  $1 - \omega$  is for the updating reputation level to evaluate the impacts of recent performance to the real-time reputation level [25].  $N_g^t$  and  $N_b^t$  denote the cumulative number of observations regarding “good” data (not false data) and “bad” data (false data) of a PMU, respectively. Correspondingly,  $\lambda_g$  and  $\lambda_b^t$  are designed as the impact factors for “good” data and “bad” data. It is natural that, from the social perspective, one needs to spend a longer period of time performing successive good behaviors to establish a high reputation level, yet only a few bad behaviors would adversely affect the reputation built over time [38]. As such, we penalize the PMUs when “bad”

#### Algorithm 2 Adaptive Reputation Updating Algorithm

---

```

1: procedure
2:   Input:  $N_g^{t-1}, N_b^{t-1}, \lambda_g, \lambda_b^{t-1}, S_b^{t-1}, \tau$ 
3:   if the judgement result of current data is “good” then
4:      $N_g^t \leftarrow N_g^{t-1} + 1$ ;
5:      $S_b^t \leftarrow 0$ ;
6:   else
7:      $N_b^t \leftarrow N_b^{t-1} + 1$ ;
8:      $S_b^t \leftarrow S_b^{t-1} + 1$ ;
9:     if  $S_b^t > 1$  then
10:        $\lambda_b^t = \lambda_b^{t-1} \cdot e^\tau$ ;
11:     end if
12:   end if
13:   Compute updating reputation level by:
14:    $T_u^t = \frac{\lambda_g \cdot N_g^t + 1}{\lambda_g \cdot N_g^t + \lambda_b^t \cdot N_b^t + 1}$ ,
15:   and the overall reputation level by:
16:    $T^t = \omega \cdot \frac{\beta}{\alpha + \beta} + (1 - \omega) \cdot \frac{\lambda_g \cdot N_g^t + 1}{\lambda_g \cdot N_g^t + \lambda_b^t \cdot N_b^t + 1}$ .
17:   Output:  $T^t$ .
18: end procedure

```

---

data are observed. In our algorithm,  $\lambda_b^t$  is designed relatively larger than  $\lambda_g$ , and  $\lambda_b^t$  will be increased if successive “bad” data are observed to amplify the impacts.

Algorithm 2 presents the ARU procedure, where  $S_b^t$  denotes the number of successive observations of “bad” data. They increment by 1 when corresponding behavior occurs. If successive “bad” data are observed, the corresponding impact factor  $\lambda_b^t$  will be increased by  $\lambda_b^{t-1} \cdot (e^\tau - 1)$ , otherwise, the counter for successive “bad” observations  $S_b^t$  will be reset to 0 and the impact factor  $\lambda_b^t$  remains unchanged. Here,  $\tau$  is initialized as a small value (e.g., 0.0001) in our experiments, and can be adjusted according to different application environments.

With the real-time reputation level of each PMU, it is easy to identify the compromised PMU by testing the following binary hypothesis:

$$\begin{cases} \mathbf{H}_0: \text{PMU } U_j \text{ is compromised,} & \text{if } T_j^t < D_{th} \\ \mathbf{H}_1: \text{PMU } U_j \text{ is not compromised,} & \text{otherwise.} \end{cases} \quad (18)$$

where  $D_{th}$  is an acceptable detection threshold. This hypothesis is tested once the reputation level is updated in order to ensure real-time detection.

## 5. Performance evaluation

In this section, we present a set of simulation experiments and the results to demonstrate the efficacy of our proposed DHCD method, including the collaborative FDD process and determination of compromised PMU process. Fig. 6 shows the IEEE 39-bus power system that is used as a benchmark system in our simulation experiments. IEEE 39-bus power system is a well-known New England power system with 10 generators, 39 buses, and 46 transmission lines, which is commonly used as a benchmark system to test and verify new schemes [22,141]. Combined with the PowerWorld simulator [5], the power system can provide real-time, accurate and precise state information of the power system. Our experiments are conducted using the PowerWorld simulator on an IEEE standard 39-bus power system, where a number of scenarios are simulated and corresponding real-time measurement data from PMUs are collected. These data are then used to evaluate our proposed DHCD method in MATLAB. The key parameters are summarized in Table 2.

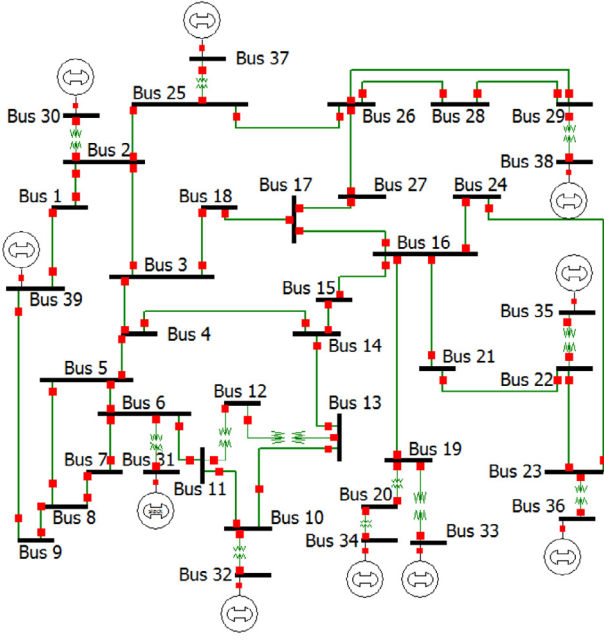


Fig. 6. IEEE 39-bus power system.

Table 2  
Simulation parameters.

Parameter	Default setting
$T_h$	0.8
$\omega$	0.4
$\lambda_g$	0.1
$\lambda_b$	0.5
$S_b$	10
$\tau$	0.001
$D_{th}$	0.6
Number of PMUs: $N$	39
Number of samples of each test: $K$	1000
State variables that collected	$\delta, V, L_{Mvar}, L_{MW}$

### 5.1. Efficacy of FDD algorithm

In this section, we simulate two groups of simulation experiments. The first group shows that only one piece of the four rule specifications is violated (with a single “1” in  $R_i^t$ ). In contrast, the second group shows that multiple pieces of the four rule specifications are violated (with multiple “1”s in  $R_i^t$ ). Further, as shown in Fig. 7, each group is divided into four different cases: (a) single, (b) sparse, (c) random, and (d) dense, representing four distribution types of false measurement data. To be specific, case (a) describes that only single PMU is inserted with false measurement data; case (b) describes that multiple sparsely distributed PMUs are inserted with false measurement data; case (c) describes that multiple randomly distributed PMUs are inserted with false measurement data; and case (d) describes that multiple densely distributed PMUs are inserted with false measurement data.

Tables 3 and 4 show the simulation results in terms of the detection rate and the average iterations of the FDD algorithm for detecting false measurement data with single violated rule and multiple violated rules, respectively. We observe from both Tables 3 and 4 that, either singly or sparsely distributed PMU(s) with inserted false measurement data can be easily detected by our FDD algorithm with a 100% detection rate. As for either randomly or densely distributed PMUs with inserted false measurement data, FDD has a high detection rate but not 100%. The reason is that, in most cases, the collaborative FDD performs well for detecting anomalous data when these corresponding PMUs are

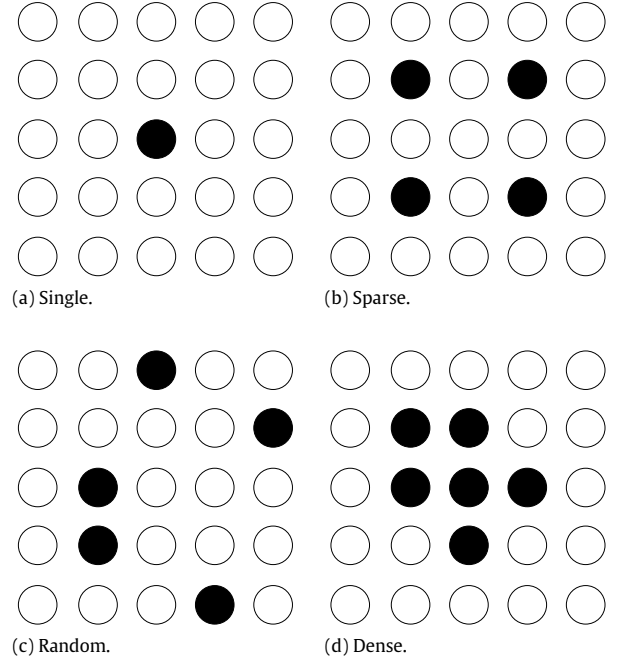


Fig. 7. Four different cases of the distribution of PMUs with inserted false measurement data: single, sparse, random, and dense.

Table 3

The detection rate and the average iterations of FDD algorithm with single rule violated false measurement data under four different distribution types. The number of PMUs with false measurement data is 6.

Distribution type	Detection rate	Average iterations
Single	100.0%	1.000
Sparse	100.0%	1.000
Random	97.1%	1.173
Dense	80.4%	2.071

Table 4

The detection rate and the average iterations of FDD algorithm with multiple rules violated false measurement data under four different distribution types. The number of PMUs with false measurement data is 6.

Distribution type	Detection rate	Average iterations
Single	100.0%	1.000
Sparse	100.0%	1.000
Random	97.9%	1.107
Dense	93.7%	1.520

located near the inner regions of the grid. The anomalies can be identified by starting from the peripheral PMUs at the first iteration to the inner PMUs at the subsequent iterations. While, in some extreme and rare cases, if these anomalous PMUs are concentrated at the marginal regions of the grid, only peripheral PMUs in the vicinity of the inner regions can be identified. After the first or two iterations, the peripheral anomalous PMUs can be identified and their connections to other PMUs removed. Therefore, other anomalous PMUs in marginal regions may be isolated with only anomalous neighboring PMUs. They can collude with each other to mutually protect each other by showing the same results  $R_i^t$ . Such extreme cases may occur in dense distribution type simulation experiments, so the dense type holds relatively lower detection rate in both group one and group two.

The average iterations for either singly or sparsely distributed PMU(s) with inserted false measurement data in both group one and group two are 1.000, as the inserted anomalous data of these two types can be easily identified by collaborative detection with only one iteration. In random distribution type, the average iterations are 1.173 and 1.107 for the two groups, respectively. This

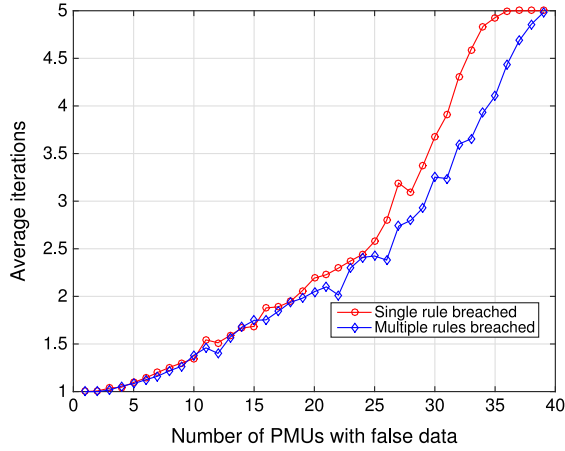


**Fig. 8.** The average iterations needed for FDD algorithm versus different numbers of PMUs with false measurement data. Two groups of false data: single rule violated and multiple rules violated are compared.

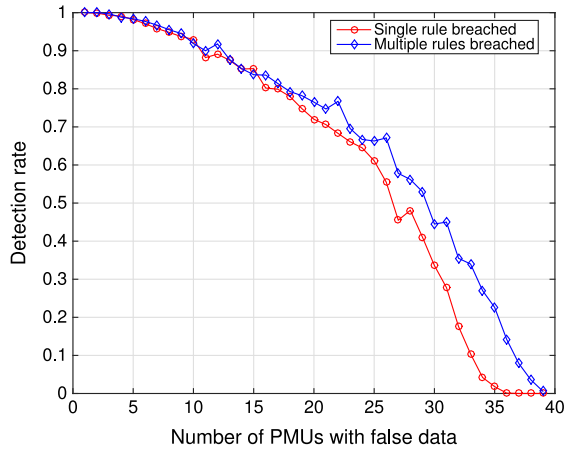


**Fig. 9.** The detection rate of FDD algorithm versus different numbers of PMUs with false measurement data. Two groups of false data: single rule violated and multiple rules violated are compared.

means that one round FDD can successfully detect the inserted false data, but in some situations, it requires another one to two rounds to detect the false data. Note that, in our simulation experiments, for undetected false data, the number of iterations is set as 5, the upper bound of FDD algorithm. As for the densely distribution type, the average iterations are 2.071 and 1.0520 respectively. This shows that, compared with random distribution type, more cases require additional FDD iterations to detect the inner false data.

Interestingly, the simulation results also show that, group two simulations can achieve a higher or equal detection rate with fewer average iterations than group one. This is because our FDD algorithm detects the false data when at least one rule is violated, so in group two it is much easier for FDD to detect the anomalous data.

In addition to the above results, we studied the relationship between the average iterations and the number of PMUs with false data under random distribution type as shown in Fig. 8, and the corresponding detection rate as well in Fig. 9. Clearly, the value of the average iterations increases, and eventually up to 5, the upper bound, as the increase in the number of PMUs with false data. Correspondingly, the value of the detection rate drops from 1 to 0 while the number of PMUs with false data increases. We also observe similar results in the sense that both values of the average iterations and the detection rate of multiple rules violation outperformed the single rule violated data.

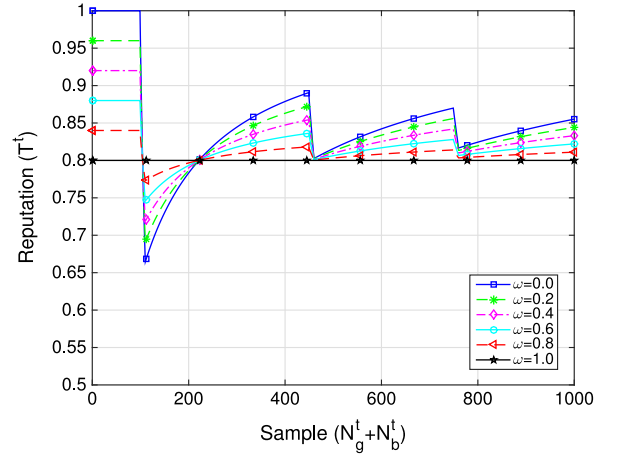


**Fig. 10.** The reputation level of a PMU under different  $\omega$ s ( $T_h = 0.8$ ,  $D_{th} = 0.6$ ,  $S_b = 10$ ,  $\lambda_b^0 = 0.5$ ).

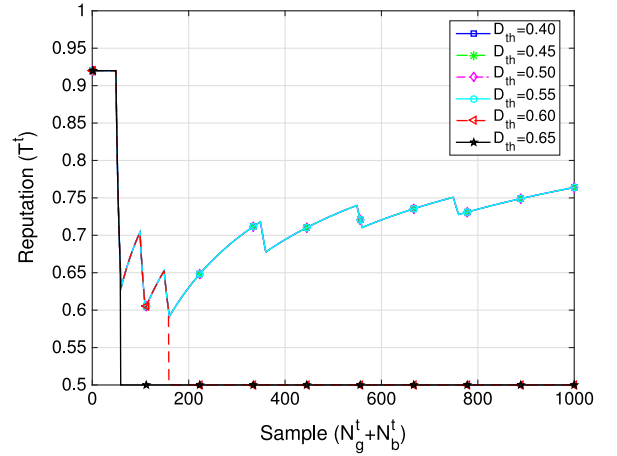


**Fig. 11.** The reputation level of a PMU under different  $D_{th}$ s ( $T_h = 0.8$ ,  $\omega = 0.4$ ,  $S_b = 10$ ,  $\lambda_b^0 = 0.5$ ).

## 5.2. Identification of compromised PMUs with Our reputation system

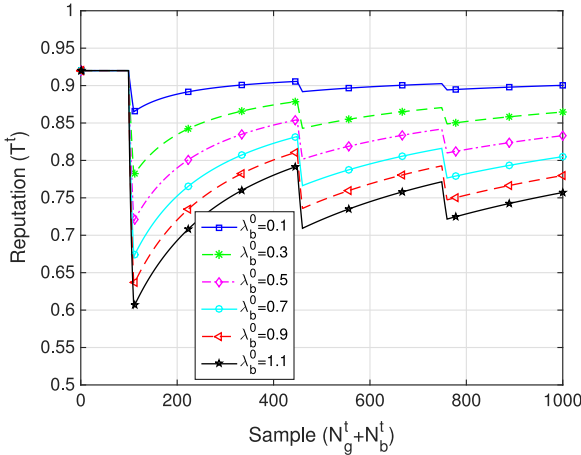
The performance of our reputation system can be affected by the following critical parameters: (1)  $\omega$ , the weight assigned for the history reputation level; (2)  $D_{th}$ , the detection threshold; (3)  $\lambda_b$ , the impact factor; and (4)  $S_b^t$ , the number of successive observations of bad data.

Fig. 10 shows the fluctuations of a PMU's reputation level under different  $\omega$ s. Three FDI events, each lasting 10 samples, are inserted into the PMU's measurement data. This figure shows that, the higher the  $\omega$  is, the more the current reputation level  $T^t$  relies on its history value  $T_h$ . Particularly,  $\omega = 0.0$  indicates that  $T^t = T_h$ , and  $\omega = 1.0$  indicates that  $T^t = T_u^t$ .

Fig. 11 shows the fluctuations of a PMU's reputation level under different  $D_{th}$ s. Six FDI events, each lasting 10 samples, are inserted into the PMU's measurement data. We observe from this figure that higher  $D_{th}$ s hold a lower tolerance to PMUs' "bad" behaviors, while lower  $D_{th}$ s have higher tolerance to PMUs' "bad" behaviors. In other words, higher  $D_{th}$ s are more sensitive than lower  $D_{th}$ s. For example, when  $D_{th} = 0.65$ , our reputation system raises an alarm when the first FDI event is inserted.

The relationship between the reputation level and the  $\lambda_b^0$  is plotted in Fig. 12. Three FDI events, each lasting 10 samples, are inserted into the PMU's measurement data. Clearly, the higher the  $\lambda_b^0$ , the more adverse the consequence of penalty to the reputation level, which means that the reputation level decreases significantly.





**Fig. 12.** The reputation level of a PMU under different  $\lambda_b^0$ s ( $T_h = 0.8$ ,  $\omega = 0.4$ ,  $D_{th} = 0.6$ ,  $S_b = 10$ ).

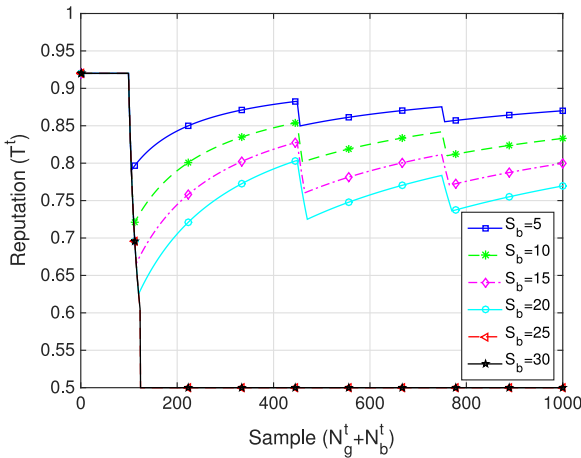


**Fig. 13.** The reputation level of a PMU under different  $S_b$  ( $T_h = 0.8$ ,  $\omega = 0.4$ ,  $D_{th} = 0.6$ ,  $\lambda_b^0 = 0.5$ ).

A similar relationship between the reputation level and the  $S_b$  is plotted in Fig. 13. Also, three FDI events but different lengths are inserted into the PMU's measurement data. Similar to Fig. 12, this figure shows that the larger the  $S_b$ , the more significance the penalty has on the reputation level, as large  $S_b$  results in more times of  $\lambda_b^t$  adjustment, i.e.,  $\lambda_b^t = \lambda_b^{t-1} * e^{\tau}$ . For instance, with  $D_{th} = 0.6$ , the reputation level drops quickly below  $D_{th}$  if  $S_b = 30$ .

## 6. Conclusions

In this paper, we proposed a novel DHCD method to identify and mitigate FDI attacks in smart grid CPS. Specifically, a rule specification based real-time collaborative detection system was designed to identify the anomalies of measurement data. In addition, a new reputation system with an ARU algorithm was presented to evaluate the overall running status of the PMUs, which can be used to identify compromised PMUs. We then demonstrated the utility of the proposed approach using simulations of the IEEE 39-bus power system.

As previously discussed, our method is designed to detect the malicious activities resulting in the anomaly of measurement data. Future work would include extending the proposed approach to capture power system faults (e.g., voltage disturbance, open circuit, and short circuit).

## References

- [1] H. Bao, R. Lu, B. Li, R. Deng, BLITHE: Behavior rule based insider threat detection for smart grid, *IEEE Internet Things J.* 3 (2) (2016) 190–205.
- [2] M.E. Baran, A.W. Kelley, State estimation for real-time monitoring of distribution systems, *IEEE Trans. Power Appar. Syst.* 9 (3) (1994) 1601–1609.
- [3] R.B. Bobba, K.M. Rogers, Q. Wang, H. Khurana, K. Nahrstedt, T.J. Overbye, Detecting false data injection attacks on DC state estimation, in: *Preprints of the First Workshop on Secure Control Systems, CPSWEEK*, Vol. 2010, 2010.
- [4] K. Bowman, L. Shenton, Parameter estimation for the Beta distribution, *J. Stat. Comput. Simul.* 43 (3–4) (1992) 217–228.
- [5] Y. Brar, J.S. Randhawa, Optimal power flow using power world simulator, in: *Proc. IEEE Electric Power and Energy Conference (EPEC)*, IEEE, 2010, pp. 1–6.
- [6] A. Castiglione, R. Pizzolante, C. Esposito, A. De Santis, F. Palmieri, A. Castiglione, A collaborative clinical analysis service based on theory of evidence, fuzzy linguistic sets and prospect theory and its application to craniofacial disorders in infants, *Future Gener. Comput. Syst.* 67 (2017) 230–241.
- [7] J. Chen, A. Abur, Placement of PMUs to enable bad data detection in state estimation, *IEEE Trans. Power Syst.* 21 (4) (2006) 1608–1615.
- [8] J. Chen, L. Shi, P. Cheng, H. Zhang, Optimal denial-of-service attack scheduling with energy constraint, *IEEE Trans. Automat. Control* 60 (11) (2015) 3023–3028.
- [9] K.-K.R. Choo, A conceptual interdisciplinary plug-and-play cyber security framework, in: *ICTs and the Millennium Development Goals*, Springer, 2014, pp. 81–99.
- [10] T.V. Cutsem, M. Ribbens-Pavell, L. Mili, Hypothesis testing identification: A new method for bad data analysis in power system state estimation, *IEEE Trans. Power Appar. Syst.* (11) (1984) 3239–3252.
- [11] C. Esposito, A. Castiglione, F. Palmieri, M. Ficco, Trust management for distributed heterogeneous systems by using linguistic term sets and hierarchies, aggregation operators and mechanism design, *Future Gener. Comput. Syst.*, in press. <http://dx.doi.org/10.1016/j.future.2015.12.004>.
- [12] N. Falliere, L.O. Murchu, E. Chien, W32. Stuxnet dossier, White paper, Symantec Corp., Security Response, 5, 2011, 6.
- [13] H. Fang, L. Xu, K.-K.R. Choo, Stackelberg game based relay selection for physical layer security and energy efficiency enhancement in cognitive radio networks, *Appl. Math. Comput.* 296 (2017) 153–167.
- [14] S. Gorman, Y.J. Dreazen, A. Cole, Insurgents hack US drones, *Wall Street J.* 17 (2009) 1–4.
- [15] E. Handschin, F. Schweppe, J. Kohlas, A. Fiechter, Bad data analysis for power system state estimation, *IEEE Trans. Power Appar. Syst.* 94 (2) (1975) 329–337.
- [16] S. Iqbal, M.L.M. Kiah, B. Dhaghghi, M. Hussain, S. Khan, M.K. Khan, K.-K.R. Choo, On cloud security attacks: A taxonomy and intrusion detection and prevention as a service, *J. Netw. Comput. Appl.* 74 (2016) 98–120.
- [17] R. Jiang, R. Lu, Y. Wang, J. Luo, C. Shen, X.S. Shen, Energy-theft detection issues for advanced metering infrastructure in smart grid, *Tsinghua Sci. Technol.* 19 (2) (2014) 105–120.
- [18] W.W. Kotiuga, M. Vidyasagar, Bad data rejection properties of weighted least absolute value techniques applied to static state estimation, *IEEE Trans. Power Appar. Syst.* (4) (1982) 844–853.
- [19] H. Kumarage, I. Khalil, Z. Tari, A. Zomaya, Distributed anomaly detection for industrial wireless sensor networks based on fuzzy data modelling, *J. Parallel Distrib. Comput.* 73 (6) (2013) 790–806.
- [20] W. Li, Risk evaluation of wide area measurement and control system, in: *Risk Assessment of Power Systems: Models, Methods, and Applications*, John Wiley & Sons, 2014, pp. 313–350.
- [21] X. Li, X. Liang, R. Lu, X. Shen, X. Lin, H. Zhu, Securing smart grid: cyber attacks, countermeasures, and challenges, *IEEE Commun. Mag.* 50 (8) (2012) 38–45.
- [22] B. Li, R. Lu, W. Wang, K.-K.R. Choo, DDOA: A Dirichlet-based detection scheme for opportunistic attacks in smart grid cyber-physical system, *IEEE Trans. Inf. Forensics Secur.* 11 (11) (2016) 2415–2425.
- [23] Y. Liu, P. Ning, M.K. Reiter, False data injection attacks against state estimation in electric power grids, *ACM Trans. Inf. Syst. Secur. (TISSEC)* 14 (1) (2011) 13.
- [24] H.M. Merrill, F.C. Schweppe, Bad data suppression in power system static state estimation, *IEEE Trans. Power Appar. Syst.* (6) (1971) 2718–2725.
- [25] F.G. Mrmol, G.M. Prez, TRIP, a trust and reputation infrastructure-based proposal for vehicular ad hoc networks, *J. Netw. Comput. Appl.* 35 (3) (2012) 934–941.
- [26] M.M. Nordman, M. Lehtonen, Distributed agent-based state estimation for electrical distribution networks, *IEEE Trans. Power Appar. Syst.* 20 (2) (2005) 652–658.
- [27] H. Otrok, N. Mohammed, L. Wang, M. Debbabi, P. Bhattacharya, A game-theoretic intrusion detection model for mobile ad hoc networks, *Comput. Commun.* 31 (4) (2008) 708–721.
- [28] F. Pasqualetti, F. Drfler, F. Bullo, Cyber-physical attacks in power networks: Models, fundamental limitations and monitor design, in: *Proc. 50th IEEE Conference on Decision and Control and European Control Conference, IEEE*, 2011, pp. 2195–2201.
- [29] A. Patel, H. Alhussian, J.M. Pedersen, B. Bounabat, J.C. Jnior, S. Katsikas, A nifty collaborative intrusion detection and prevention architecture for smart grid ecosystems, *Comput. Secur.* 64 (2017) 92–109.
- [30] J. Peng, K.-K.R. Choo, H. Ashman, User profiling in intrusion detection: A review, *J. Netw. Comput. Appl.* 72 (2016) 14–27.
- [31] U.S. Premaratne, I. Khalil, M. Atiquzzaman, Trust based reliable transmissions strategies for smart home energy consumption management in cognitive radio based smart grid, *Ad Hoc Networks* 41 (2016) 15–29.

- [32] M. Qiu, W. Gao, M. Chen, J.-W. Niu, L. Zhang, Energy efficient security algorithm for power grid wide area monitoring system, *IEEE Trans. Smart Grid* 2 (4) (2011) 715–723.
- [33] M. Qiu, H. Su, M. Chen, Z. Ming, L.T. Yang, Balance of security strength and energy for a PMU monitoring system in smart grid, *IEEE Commun. Mag.* 50 (5) (2012) 142–149.
- [34] S. Rajasegarar, C. Leckie, M. Palaniswami, Hyperspherical cluster based distributed anomaly detection in wireless sensor networks, *J. Parallel Distrib. Comput.* 74 (1) (2014) 1833–1847.
- [35] F.C. Schweppe, J. Wildes, D.B. Rom, Power system static-state estimation, parts I, II, and III, *IEEE Trans. Power Appar. Syst.* 89 (1) (1970) 120–135.
- [36] S. Shin, G. Gu, Conficker and beyond: A large-scale empirical study, in: *Proc. 26th Annual Computer Security Applications Conference, ACSAC, 2010*, pp. 151–160.
- [37] M. Srivatsa, L. Xiong, L. Liu, Trustguard: countering vulnerabilities in reputation management for decentralized overlay networks, in: *Proc. 14th International Conference on World Wide Web, (WWW), ACM, 2005*, pp. 422–431.
- [38] Y.L. Sun, Z. Han, W. Yu, K.J.R. Liu, A trust evaluation framework in distributed networks: Vulnerability analysis and defense against attacks, in: *Proc. IEEE INFOCOM, 2006*, pp. 1–13.
- [39] M. Xie, S. Han, B. Tian, S. Parvin, Anomaly detection in wireless sensor networks: A survey, *J. Netw. Comput. Appl.* 34 (4) (2011) 1302–1325.
- [40] L. Xie, Y.L. Mo, B. Sinopoli, False data injection attacks in electricity markets, in: *Proc. First IEEE International Conference on Smart Grid Communications, SmartGridComm, 2010*, pp. 226–231.
- [41] D. Zhang, S. Li, P. Zeng, C. Zang, Optimal microgrid control and power-flow study with different bidding policies by using powerworld simulator, *IEEE Trans. Sustainable Energy* 5 (1) (2014) 282–292.



**Beibei Li** received the B.E. degree in communication engineering from Beijing University of Posts and Telecommunications, Beijing, China, in 2014. He is currently a Ph.D. student with the INFINITUS Laboratory, School of Electrical and Electronic Engineering, Nanyang Technological University, Singapore. His research interests include cyber-physical system security and applied cryptography.



**Rongxing Lu** has been an assistant professor at the Faculty of Computer Science, University of New Brunswick (UNB), Canada, since August 2016. Before that, he worked as an assistant professor at the School of Electrical and Electronic Engineering, Nanyang Technological University (NTU), Singapore from May 2012 to August 2016. Rongxing Lu worked as a Postdoctoral Fellow at the University of Waterloo from May 2012 to April 2013. He was awarded the most prestigious “Governor General’s Gold Medal”, when he received his Ph.D. degree from the Department of Electrical and Computer Engineering, University of Waterloo, Canada, in 2012; and won the 8th IEEE Communications Society (ComSoc)

Asia Pacific (AP) Outstanding Young Researcher Award, in 2013. He is presently a senior member of IEEE Communications Society. His research interests include applied cryptography, privacy enhancing technologies, and IoT-Big Data security and privacy. He has published extensively in his areas of expertise (with more than 7500 citations from Google Scholar), and was the recipient (with his students and colleagues) of the Student Best Paper Award, ITS Summit Singapore 2015, the IEEE IES Student Best Paper Award 2014, the Best Paper Awards of TSINGHUA Science and Technology Journal 2014, IEEE ICC 2015, IEEE WCNC 2013, BodyNets 2010, and IEEE ICCCN 2009. He was/is on the editorial boards of several international referred journals, e.g., IEEE NETWORK, and currently serves the technical symposium co-chair of IEEE GLOBECOM’16, and many technical program committees of IEEE and others international conferences, including IEEE INFOCOM and ICC. In addition, he is currently organizing a special issue on “security and privacy issues in fog computing” in Elsevier Future Generation Computer Systems and a special issue on “big security challenges in big data era” in IEEE INTERNET OF THINGS JOURNAL. Dr. Lu currently serves as the Secretary of IEEE ComSoc CIS-TC (Communications and Information Security Technical Committee).



**Wei Wang** received the B.Eng. degree in Information Countermeasure Technology and the M.S. degree in Signal and Information Processing from Xidian University in 2011 and 2014, respectively. He is currently pursuing the Ph.D. degree in Electrical and Electronic Engineering at Nanyang Technological University, Singapore. His research interests include cooperative communications, cognitive radios and physical layer security.



**Kim-Kwang Raymond Choo** received the Ph.D. in Information Security in 2006 from Queensland University of Technology, Australia. He currently holds the Cloud Technology Endowed Professorship at The University of Texas at San Antonio, and is an associate professor at University of South Australia. He has served as the Special Issue Guest Editor of ACM Transactions on Embedded Computing Systems (2016; DOI: [10.1145/3015662](https://doi.org/10.1145/3015662)), ACM Transactions on Internet Technology (2016; DOI: [10.1145/3013520](https://doi.org/10.1145/3013520)), Digital Investigation (2016; DOI: [10.1016/j.diin.2016.08.003](https://doi.org/10.1016/j.diin.2016.08.003)), Future Generation Computer Systems (2016; DOI: [10.1016/j.future.2016.04.017](https://doi.org/10.1016/j.future.2016.04.017)), IEEE Cloud (2015; DOI: [10.1109/MCC.2015.84](https://doi.org/10.1109/MCC.2015.84)), IEEE Network (2016; DOI: [10.1109/MNET.2016.7764272](https://doi.org/10.1109/MNET.2016.7764272)) Journal of Computer and System Sciences (2017; DOI: [10.1016/j.jcss.2016.09.001](https://doi.org/10.1016/j.jcss.2016.09.001)), Multimedia Tools and Applications (2017; DOI: [10.1007/s11042-016-4081-z](https://doi.org/10.1007/s11042-016-4081-z)), Pervasive and Mobile Computing (2016; DOI: [10.1016/j.pmcj.2016.10.003](https://doi.org/10.1016/j.pmcj.2016.10.003)), etc. He is the recipient of various awards including ESORICS 2015 Best Paper Award, Winning Team of the Germany’s University of Erlangen-Nuremberg (FAU) Digital Forensics Research Challenge 2015, and 2014 Highly Commended Award by the Australia New Zealand Policing Advisory Agency, Fulbright Scholarship in 2009, 2008 Australia Day Achievement Medallion, and British Computer Society’s Wilkes Award in 2008. He is a Fellow of the Australian Computer Society, and a Senior Member of IEEE.